FEBS Letters 582 (2008) 2601–2608

The effect of MinC on FtsZ polymerization is pH dependent and can be counteracted by ZapA

Dirk-Jan Scheffers*,[1]

Department of Molecular Microbiology, Institute of Molecular Cell Biology, VU University Amsterdam, De Boelelaan 1085, The Netherlands

Received 30 May 2008; revised 16 June 2008; accepted 17 June 2008

Available online 25 June 2008

Edited by Stuart Ferguson

Abstract The *min* system prevents polar cell division in bacteria. Here, the biochemical characterization of the interaction of MinC and FtsZ from a Gram-positive bacterium, *Bacillus subtilis*, is reported. *B. subtilis* MinC inhibits FtsZ polymerization in a pH-dependent manner by preventing the formation of lateral associations between filaments. The inhibitory effect of MinC on FtsZ polymerization is counteracted by the presence of ZapA, a protein that promotes FtsZ filament bundling.

Keywords: Cell division; FtsZ; MinC; ZapA; GTP hydrolysis; FtsZ polymerization

1. Introduction

Rod shaped bacteria divide precisely in the middle by forming a transverse septum that divides a cell into two daughter cells. Cell division starts with self-assembly of the bacterial tubulin homologue FtsZ into a ring-like structure at midcell [1,2]. FtsZ ring formation is subject to tight control to ensure that cell division takes place at the right place and the right time. Two systems ensure correct FtsZ ring positioning: the Min system and nucleoid occlusion [3]. The Min system, originally identified in *Escherichia coli* [4], prevents division at the cell poles. In the absence of *min*, polar division gives rise to spherical minicells that lack chromosomal DNA and elongated cells that contain two nucleoids.

The Min system consists of a set of proteins that act together to prevent division at cell poles [3]. The core of the system consists of MinC and MinD which form a dimer of dimers that binds to the cytoplasmic membrane. MinC is the inhibitor of FtsZ polymerization [5], whereas MinD mediates membrane binding in an ATP regulated fashion [6–8]. Topological specificity to the MinCD inhibitor is conferred by a third protein which differs between Gram-positive (DivIVA) and Gram-negative bacteria (MinE)[3]. In Gram-positives, DivIVA localises to cell poles and keeps MinCD anchored to the poles [9,10] whereas in Gram-negatives, MinE imposes a pole-to-pole oscillation on MinCD [6–8,11,12]. The net result of both DivIVA and MinE activity is that the concentration of MinCD is lowest at midcell. Cell elongation causes the midcell concentration of MinCD to drop below a threshold that allows assembly of the FtsZ ring (e.g. 13,14).

MinC, the actual inhibitor of FtsZ, functions as a dimer [5]. In vitro experiments, in which *E. coli* FtsZ and a MalE-MinC fusion were mixed, showed concentration dependent inhibition of FtsZ polymerization, with near complete inhibition at a 1:1 ratio of FtsZ to MinC. MinC did not affect FtsZ GTPase activity [5]. This suggests that MinC affects assembly of short FtsZ oligomers into long filaments and/or filament bundling as GTP hydrolysis requires the interaction of at least two FtsZ monomers [15]. MinC consists of an N-terminal 'Z-domain' that interacts with FtsZ and prevents FtsZ polymerization in vitro, and a C-terminal 'D-domain' required for MinD binding; both domains are involved in MinC self-association [16]. Recently, it was reported that the C-terminal domain of MinC, when overexpressed, also inhibits formation of the FtsZ ring in vivo [17] and prevents lateral interactions between FtsZ filaments in vitro [18]. Despite the fact that crystal structures of both MinC [19] and several FtsZ species [20] exist, it is not known how FtsZ and MinC interact.

It is generally assumed that the MinCD action is conserved between species, although only the effect of *E. coli* MinC on FtsZ has been characterized in detail [5]. Generally, MinC is a lot less conserved than MinD, with sequence similarity between *Bacillus subtilis* and *E. coli* MinC and MinD 39% and 67%, respectively [3]. In this report the effects of *B. subtilis* MinC on FtsZ polymerization are characterized.

2. Materials and methods

2.1. Strains, plasmids, growth conditions

Strains and plasmids are listed in Table 1. DNA manipulations were carried out using standard methods [21]. Liquid medium was Luria Bertani broth (LB), solid medium was LB with 1.5% w/v agar, with antibiotics and glucose (0.5% w/v) added as required. Ampicillin was used at 100 μg/ml, spectinomycin at 50 μg/ml.

2.2. Plasmid construction

For plasmid pSG5331, *minC* was amplified from chromosomal DNA from *B. subtilis* strain 168 by PCR using primers JBJ1 and JBJ2 (primers listed in Table 1). The PCR product was digested with SalI and EcoRI and ligated into SalI/EcoRI digested pMalc2 (New England Biolabs). For plasmid pDJ15 *minC* was amplified from chromosomal DNA from strain 168 by PCR using primers DJS261 and DJS262. The PCR product was digested with *Bsa*I and ligated into *Bsa*I digested pASK-IBA3 (IBA GmbH). pDJ15 was used as a

*Fax: +31 20 5987155.
E-mail addresses: dirk-jan.scheffers@falw.vu.nl, djscheffers@itqb.unl.pt (D.-J. Scheffers).

[1]Present address: Bacterial Membrane Proteomics Laboratory, Instituto de Tecnologia Química e Biológica, Avenida da República, 2781-901, Oeiras, Portugal.

0014-5793/$34.00
doi:10.1016/j.febslet.2008.06.038

Table 1
Strains, plasmids and primers

	Relevant characteristics	Reference
Strains		
Bacillus subtilis		
168	*trpC2*	Laboratory collection
Escherichia coli		
BL21 (DE3)		[32]
DH5α	F-*endA1 hsdR17 supE44 thi-1 λ-recA1 gyrA96 relA1* Δ (*lacZYA-argF*)*U169* Φ *80 dlacZ* Δ *M15*	GIBCO-BRL
Plasmids		
pCXZ	*bla* P_{tac}-$ftsZ_{BS}$	[22]
pBS58	*spc* $ftsQAZ_{EC}$	[22]
pMal-c2	*bla* $lacI^{Q}P_{tac}$-*malE*-MCS[a]-*lacZ* α	New England Biolabs
pET21d	*bla* $lacI^{Q}P_{T7}$-MCS-his_6	Novagen
pASK-IBA3	*bla tetR PtetA*-MCS-*strep-tagII*	IBA GmbH
pSG5331	*bla* $lacI^{Q}P_{tac}$-*malE-minC*	This work
pSG1154	*bla amyE3′ spc* P_{xyl}-MCS-*gfpmut1 amyE5′*	[33]
pDJ15	*bla tetR PtetA-minC-strep-tagII*	This work
pDJ16	*bla tetR PtetA-minC19-strep-tagII*	This work
pDJ26	*bla* $lacI^{Q}P_{T7}$-his_8-*zapA*	This work
Primers	5′–3′ sequence, restriction site underlined	*Restriction enzyme*
JBJ1	GTCGTCGAATTCATGAAGACCAAAAAGCAGC	EcoRI
JBJ2	GACGACGTCGACTCACATTCCTCCCTCAAG	SalI
DJS261	CTCCTCGGTCTCCAATGAAGACCAAAAAGCAGC	BsaI
DJS262	GAGGAGGGTCTCAGCGCTCATTCCTCCCTCAAGCCTTG	BsaI
DJS266	GTAACAATAAAAGACACAAAGAATGGACTAACATTGCATCTGGATGATGCG	
DJS267	CTTTGTGTCTTTTATTGTTACATATTGCTGCTTTTTGGTCTTCACAATATTCA	
DJS297	GAGGAGGAATTCTCAATCCTTTTCTTTAAGCTG	EcoRI
DJS298	CTCTCCTCCATGGCCCATCACCATCACCATCACCATCACGGTTCCATGTCTGACGGCAAAAAAACA	NcoI

[a]MCS: multiple cloning site.

template for site directed mutagenesis (Quickchange, Stratagene) to introduce the *minC19* (G13D) mutation with primers DJS266 and DJS267 to generate pDJ16.

For plasmid pDJ26 *zapA* was amplified from chromosomal DNA from strain 168 by PCR using primers DJS297 and DJS298. The PCR product was digested with NcoI and EcoRI and ligated into NcoI/EcoRI digested pET21d (Novagen).

2.3. Protein purification and size exclusion chromatography

All proteins were purified as described earlier [5,22] or using standard protocols for tagged proteins, as described in Supplementary material. Protein concentrations were determined using the Bio-Rad Dc protein assay.

Aliquots of MinC-strep and MinC19-strep (0.2 mg protein total) were analysed by size exclusion chromatography on a Superose 12 HR10/30 column (Amersham Biosciences) run in 50 mM HEPES; 100 mM NaCl; 1 mM EDTA, pH 8.0. The column was calibrated with albumin (67 kDa), ovalbumin (47 kDa), chymotrypsinogen (25 kDa) and ribonucleaseA (14 kDa) run under identical conditions.

2.4. FtsZ sedimentation assay

FtsZ sedimentation was essentially performed as described [23]. FtsZ and additional proteins were incubated for 5 min at 30 °C in a total of 45 μl polymerization buffer with 10 mM $MgCl_2$. Various polymerization buffers were used: MES, pH 6.5 (50 mM MES/NaOH; pH 6.5; 50 mM KCl); Pipes, pH 6.8 (25 mM Pipes/NaOH; pH 6.8); HEPES, pH 7.0 (50 mM HEPES/NaOH; pH 7.0; 50 mM KCl); HEPES, pH 7.5 (50 mM HEPES/NaOH; pH 7.5; 50 mM KCl). When both ZapA and MinC were included in the assay FtsZ was added last to avoid association of FtsZ to either MinC or ZapA alone before the other protein was present. Buffer effects were excluded by inclusion of protein storage buffer to similar volumes as the maximum amount of proteins added. Polymerization was started by the addition of 5 μl 10 mM GTP or GDP and samples were incubated 5 or 20 min at 30 °C. When required, 0.5 μl diethylaminoethyl(DEAE)-dextran (10 mg/ml) was added, 10 μl samples were withdrawn (totals) and 30 μl of the polymerization reaction was spun down (10 min; 285000 × *g*; 20 °C). The supernatant fraction was withdrawn and the pellet was resuspended with 30 μl SDS–PAGE sample buffer. The amount of FtsZ present in the fractions was determined by SDS–PAGE, Coomassie Brilliant Blue staining and densitometric scanning.

2.5. GTP hydrolysis assay

FtsZ and MinC-strep (concentrations indicated in the text) were incubated at 30 °C in polymerization buffer with 10 mM $MgCl_2$. Buffer effects were excluded by inclusion of MinC storage buffer to a similar volume as the maximum amount of MinC-strep added. GTP was added to 1 mM and at different time points during a 30 min interval, 30 μl samples were withdrawn, released phosphate was detected with malachite green and GTP hydrolysis was calculated as GTP turnover per FtsZ molecule per minute [15]. Each experiment was performed three times; the mean result and standard deviation are plotted.

2.6. Light scattering

Light scattering experiments were performed using an Aminco Bowman Series 2 spectrometer (SLM Instruments) as described [23]. Excitation and emission wavelengths were set to 350 nm, with slit widths of 2 nm, and the photomultiplier tube at 500 V. Protein (concentrations indicated in the text) was incubated in 300 μl of polymerization buffer with 10 mM $MgCl_2$, in a fluorescence cuvette with a 1 cm path length. Buffer effects were excluded by inclusion of MinC storage buffer to a similar volume as the maximum amount of MinC-strep added. The sample was maintained at 30 °C. After 3 min of data collection, GTP was added to 1 mM, with a maximum sample volume increase of 10%.

2.7. Negative stain electron microscopy

FtsZ polymerization was performed as described for the sedimentation assay. A 2 μl aliquot of the polymerization reaction was applied to a 400 mesh carbon-coated copper grid (Electron Microscopy Sciences). The grid was blotted dry and negatively stained for 1 min by applying 1 μl of a 1% uranyl-acetate solution. The grids were viewed in a JEOL JEM1010 transmission electron microscope.

3. Results

3.1. MinC inhibition of FtsZ polymerization is pH dependent

I set out to reconstitute *B. subtilis* FtsZ polymerization in vitro in the presence of a MalE-MinC fusion protein as previously described for *E. coli* FtsZ and MinC [5]. Initial experiments revealed that although a MalE–MinC fusion is

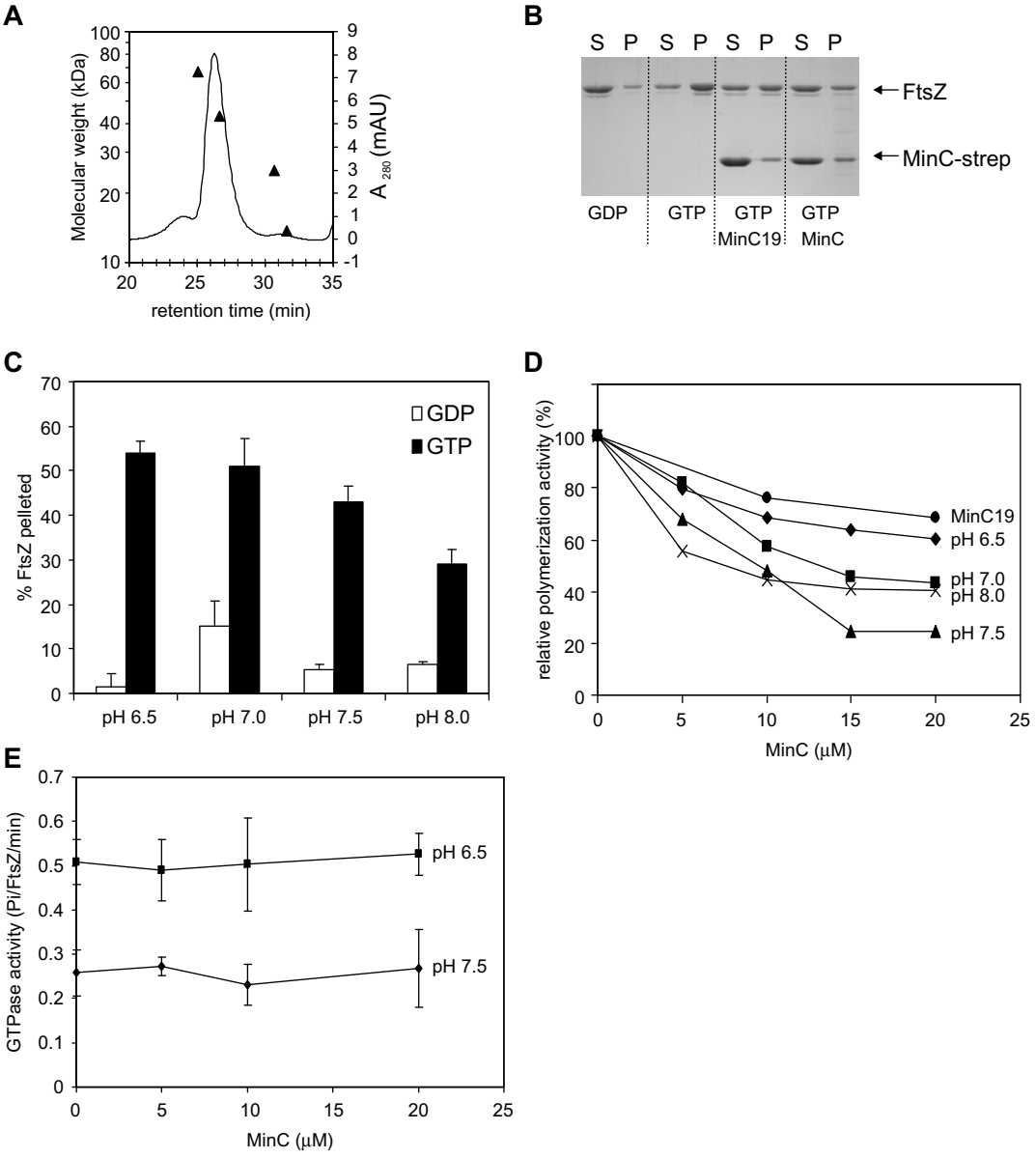

Fig. 1. Inhibitory effect of MinC on polymerization and GTPase of FtsZ. (A) Size exclusion chromatography of MinC-strep on a Superose12 HR10/30 column. The MinC-strep elution profile is shown, with positions of Molecular weight standards (see Section 2) indicated by filled triangles. (B) Sedimentation assay. FtsZ (10 μM) was incubated with 1 mM nucleotide and MinC19-strep or MinC-strep (20 μM) for 5 min and polymers were spun down by centrifugation. Equal volumes of the supernatant (S) and pellet (P) fractions were analysed by SDS–PAGE. (C) Quantification of FtsZ polymerization at different pH values as analysed by sedimentation. GDP serves as a control for aspecific sedimentation. (D) Relative inhibition of FtsZ polymerization by MinC-strep at different pH values. FtsZ (10 μM) was polymerized with 1 mM GTP in the presence of MinC-strep or MinC19-strep and polymers were spun down by centrifugation. The amount of FtsZ pelleted in the absence of MinC-strep was set at 100%. The MinC19-strep experiment depicted was performed at pH 7.5; similar results were obtained at other pH values (not shown). (E) The effect of MinC on FtsZ GTPase activity. FtsZ (10 μM) GTPase activity was determined in MES, pH 6.5, and HEPES, pH 7.5, polymerization buffers, with MinC at concentrations indicated. The results in C and D and E represent the mean of at least three independent experiments.

capable of inhibiting FtsZ polymerization, MalE alone also inhibited FtsZ polymerization and co-sedimented with FtsZ, suggesting that MalE by itself has a negative effect on *B. subtilis* FtsZ polymerization (Fig. S1). Next, a C-terminal strep-tag, adding only 10 amino acid residues, was used to purify *B. subtilis* MinC. Purified MinC-strep eluted as a single peak consistent with a dimer during size-exclusion chromatography (Fig. 1A; calculated Mw 52.4 kDa, estimated Mw from retention time 53.1 kDa), similar to C-terminally His_6-tagged, functional, *E. coli* MinC [19]. As a control for specificity of MinC-strep the conserved Glycine at position 13 was mutagenized to Aspartate. This mutation is equivalent to the *E. coli* MinC19 mutation that has a reduced affinity for FtsZ and a reduced capacity to inhibit FtsZ polymerization in vitro [5]. *B. subtilis* MinC(G13D)-strep purified as a dimer similar to wild type MinC-strep (not shown) and will be called MinC19-strep in the rest of this paper. In a sedimentation assay, MinC-strep had an inhibitory effect on FtsZ polymerization, whereas MinC19-strep did not inhibit FtsZ polymerization to the same extent, as would be expected if the mutation of

the conserved glycine had a similar effect (Fig. 1B). Surprisingly, a considerable amount of polymerized FtsZ (60% of the maximum) was still found in the pellet fraction when MinC-strep was present in 2-fold molar excess. Previously, almost complete inhibition of FtsZ polymerization by MalE-MinC at a 1:1 ratio was reported for the *E. coli* proteins using similar buffer conditions [5]. Therefore, the polymerization reaction was investigated in more detail. First, FtsZ sedimentation was determined over a pH range of 6.5–8.0 using MES (pH 6.5) and HEPES (pH 7.0; 7.5 and 8.0) as buffering agents, with KCl at 50 mM and $MgCl_2$ at 10 mM in all experiments. The amount of FtsZ polymers that could be sedimented was reduced with increased pH (Fig. 1C), similar to *E. coli* FtsZ [24]. Next, the sedimentation assay was carried out at different pH values, with MinC-strep at varying concentrations. At higher pH values MinC-strep displayed a clear, concentration dependent, inhibition of FtsZ polymerization with maximum inhibition at pH 7.5 (Fig. 1D). In contrast, FtsZ polymerization in the presence of 2 fold excess MinC19-strep was never lower than 68% of the original level (Fig. 1D, not shown). Comparison of FtsZ GTPase activity at pH 6.5 and pH 7.5 revealed a decrease in GTPase activity at the higher pH (Fig. 1E). MinC-strep did not affect GTPase activity at either pH, similar to what was reported for *E. coli* MinC (Fig. 1E) [5].

In the sedimentation assay, DEAE-dextran is included to promote efficient sedimentation of the polymers (see e.g. 25), and in sedimentation experiments performed in the absence of DEAE-dextran no polymerized FtsZ could be recovered in the pellet (not shown). An alternative sedimentation protocol that does not require the inclusion of DEAE-dextran for sedimentation uses a Pipes buffer (pH 6.8) [26]. Using this protocol, relatively high amounts of FtsZ sedimented in the presence of GDP, and more importantly, MinC-strep was not active for inhibition of FtsZ polymerization but rather co-sedimented with FtsZ (Fig. S2). Because of these results, and the finding that the presence of Pipes itself can promote polymerization of the FtsZ homologue tubulin [27] the Pipes buffer was not used in further experiments.

To confirm the sedimentation results, FtsZ polymerization and bundling was monitored by light scattering and electron microscopy (EM) at pH 6.5 and 7.5. Light scattering is a very direct assay to monitor the dynamics of FtsZ polymerization but is only semi-quantitative with respect to the amount of protein present in polymers as the extent of filament bundling greatly influences the scattering signal [24]. EM provides information about the structure of the filaments. At pH 6.5, FtsZ polymerization and bundling upon GTP addition was immediate (Fig. 2A), and MinC-strep inhibited FtsZ polymerization to a similar extent as observed with sedimentation. EM

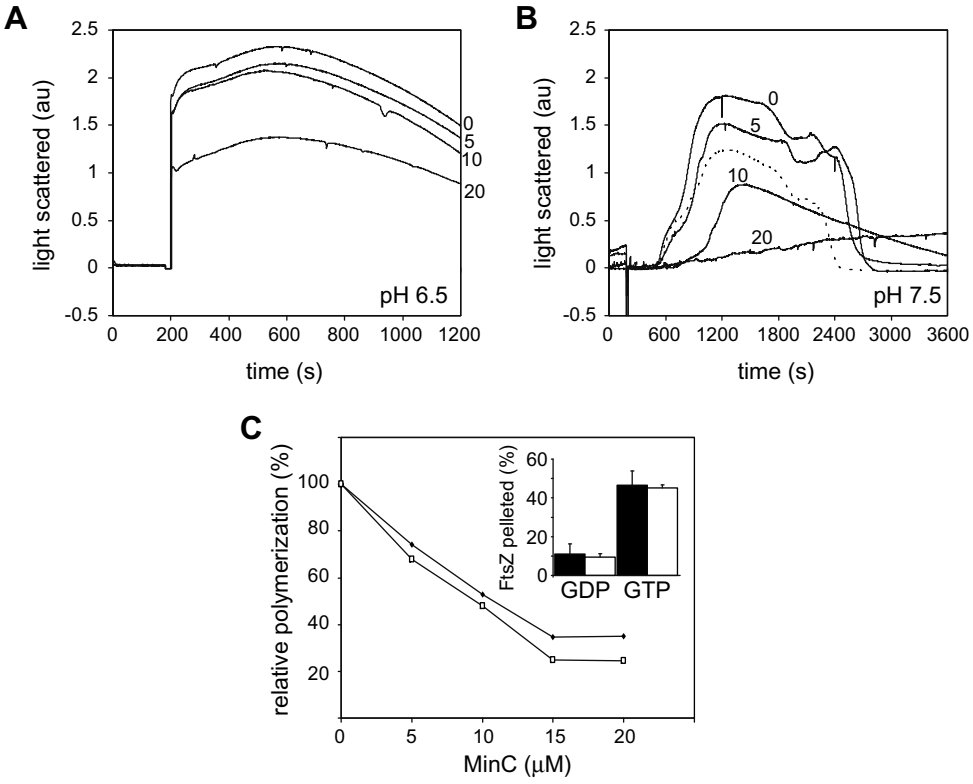

Fig. 2. Dynamics of FtsZ polymerization and inhibition by MinC at pH 6.5 and pH 7.5. (A, B) Light scattering assay. FtsZ (10 μM) was incubated in polymerization buffer with MinC-strep (concentration in μM indicated to the right end of the curves [A] or next to the curves [B] for clarity). After 3 min. baseline recording, GTP was added to 1 mM. Dashed line (B) shows a control experiment with MinC19-strep (20 μM). Note the difference in timescales between (A) and (B). Spectrophotometer settings were equal for all experiments, but baseline signals were corrected for levels immediately after GTP addition in (B) (see text, Table 2). (C) Relative inhibition of FtsZ polymerization by MinC-strep at pH 7.5 after different polymerization times. FtsZ (10 μM) was polymerized with 1 mM GTP in the presence of MinC-strep for 5 min (open symbols) or 20 min (closed symbols) and polymers were spun down by centrifugation. The amount of FtsZ pelleted in the absence of MinC-strep was set at 100%. The inset shows the absolute amounts of FtsZ pelleted in this experiment in the absence of MinC-strep with sedimentation after 5 min (open bars) or 20 min (closed bars).

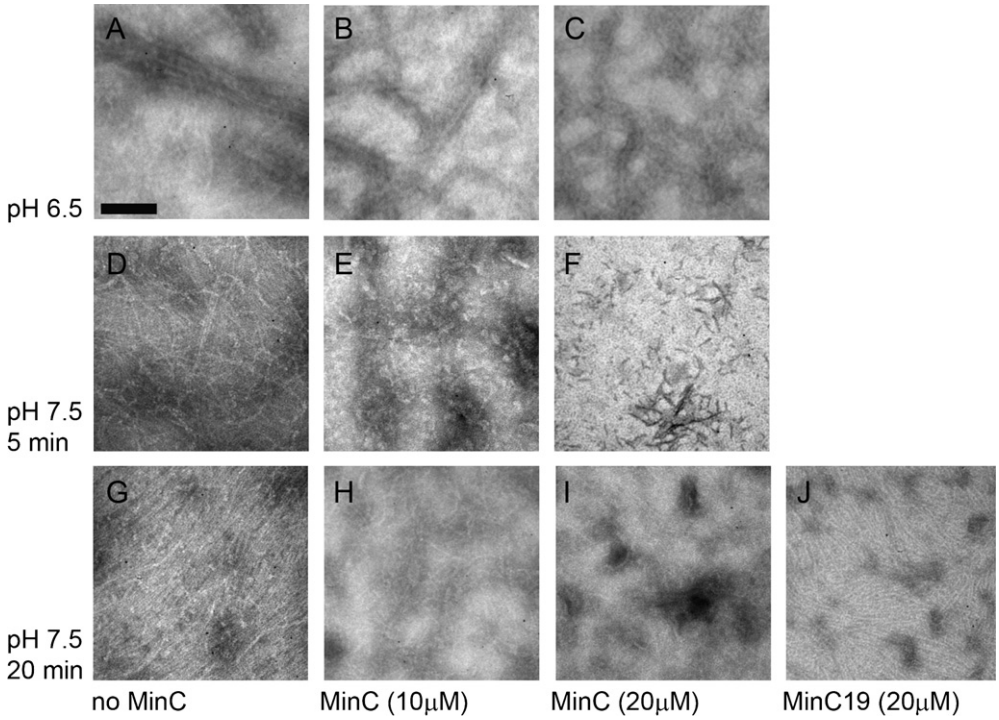

Fig. 3. Electron microscopy of FtsZ polymers. FtsZ (10 μM) was polymerized and prepared for electron microscopy as described in the text. Reactions were performed in the absence (A, D, G) or presence of 10 μM (B, E, H) or 20 μM (C, F, I) of MinC-strep or 20 μM of MinC19-strep (J). Scale bar 100 nm.

revealed that FtsZ filaments seemed less bundled when MinC-strep was present (Fig. 3A–C).

At pH 7.5 a striking difference was observed. The presence of MinC-strep increased the baseline signal considerably in the light scattering assay in a concentration-dependent manner (Table 2). This increase in scatter signal points at the formation of protein–protein complexes, either by FtsZ and MinC-strep or MinC-strep alone, in a pH-dependent fashion. Notably, the baseline signal increase was pH dependent and was considerably lower when MinC19-strep was added. For clarity, scatter signals immediately after GTP addition were set to 0 to allow comparison of the effect of MinC-strep on polymerization (Fig. 2B). At higher concentrations of MinC-strep the addition of GTP caused a slight drop in the light scattering signal. At pH 7.5, the light scattering signal did not increase immediately upon the addition of GTP, and signal increase seemed to be delayed even more in the presence of MinC-strep. Light scattering signals were maximal ~20 min after addition of GTP, and the amplitude of the signal decreased with an increase in MinC-strep concentration similar to what was observed in the sedimentation experiment. Note that as in sedimentation, the maximum amount of signal in scattering was higher at pH 6.5 then at pH 7.5. As the initial sedimentation experiment at pH 7.5 was carried out 5 min after the addition of GTP and therefore may have missed maximum polymerization, the sedimentation experiment was repeated with a 20 min incubation time. This gave essentially the same results for both maximum amount of FtsZ polymerized and inhibition by MinC (Fig. 2C). Examination of the polymerization reactions after 5 and 20 min by EM revealed that after 5 min FtsZ filaments are visible at pH 7.5 which seem to have organized in lateral arrays, rather than bundles, after 20 min (Fig. 3D and G). The presence of MinC-strep hindered (10 μM) or blocked (20 μM) formation of these filaments after 5 min, but after 20 min filaments could be observed in all reactions (Fig. 3E, F, H and I). Filaments formed in the presence of MinC-strep appeared shorter and more curved, and arrays of long filaments parallel to each other were not found. In contrast, the presence of 20 μM MinC19-strep did not affect the formation of long filaments that run in lateral arrays (Fig. 3J). The fact that FtsZ polymers are observed by EM after 5 min (Fig. 3D) and can be sedimented in the presence of DEAE after 5 min (Fig. 2C), suggests that the light scattering signal increase is predominantly caused by bundling or formation of lateral arrays of FtsZ protofilaments.

Table 2
Absolute baseline levels (arbitrary units) in light scattering experiments shown in Fig. 2A and B

MinC-strep	MES, pH 6.5	HEPES, pH 7.5
0 μM	0.03	0.09
5 μM	0.03	0.30
10 μM	0.03	0.97
20 μM	0.03	1.73
20 μM MinC19-strep	ND[a]	0.13

[a]ND: not determined.

3.2. ZapA counteracts the effect of MinC in vitro

ZapA is a protein that stabilizes FtsZ polymers by promoting FtsZ bundling through a direct interaction with FtsZ, possibly through cross-linking FtsZ filaments [28,29]. In vivo ZapA counteracts the inhibitory effect of MinCD [28]. To

study whether the in vivo effect of ZapA can be reproduced in vitro, His_8-ZapA was purified and included in FtsZ polymerization assays in the presence or absence of MinC-strep. Polymerization assays were performed in HEPES pH 7.5 with 20 min polymerization time to allow for maximal polymerization. Consistent with previous observations [28,29], the addition of His_8-ZapA to sedimentation assays precluded the need for DEAE-dextran for efficient sedimentation, as His_8-ZapA bundled the FtsZ polymers. At a 1:1 ratio of His_8-ZapA to FtsZ, the amount of FtsZ recovered in the pellets is similar to that when DEAE-dextran is added to the reaction mixture (Fig. 4A), and extensive bundling can be observed (Fig. 4C). At a ZapA:FtsZ ratio of 1:2, the total amount of FtsZ recovered was reduced (Fig. 4A). Strikingly, the inclusion of MinC (up to a FtsZ:MinC-strep ratio of 1:2) had no effect on the amount of FtsZ recovered when His_8-ZapA was present, irrespective of the FtsZ:ZapA ratio (Fig. 4A). Again, MinC-strep did not co-sediment with FtsZ (Fig. 4B), whereas ZapA was found to co-sediment with FtsZ as described [29]. EM corroborated these results: in the presence of His_8-ZapA, FtsZ polymers formed thick bundles, and polymer length and bundling were not affected by MinC (Fig. 4C–E). Similar results were obtained when the experiment was performed in MES, pH 6.5 (not shown). This result shows that ZapA directly counteracts, or protects FtsZ from, the inhibitory effect of MinC.

4. Discussion

In this study the biochemical characterization of the inhibition of FtsZ activity by MinC from a Gram-positive bacterium, *B. subtilis*, is reported. Like previously reported for *E. coli* MinC [5], *B. subtilis* MinC is capable of inhibiting FtsZ polymerization, but the effect is strikingly pH dependent. Initial polymerization experiments were performed in a MES buffer at pH 6.5 which is commonly used for polymerization studies of FtsZ from both *B. subtilis* and *E. coli* (e.g. [18,23,25]). Using these conditions only a mild inhibition of FtsZ polymerization by MinC-strep was observed. The effect of MinC became stronger when the pH was raised above 7.0. As the internal pH of *B. subtilis* is in the range of 7.0–8.5 at an external pH range of 5–8 [30], the pH dependence observed suggests that *B. subtilis* MinC has evolved for maximal activity at pH values that are encountered in vivo. The results indicate that pH dependence is an important factor that must be taken into consideration when studying FtsZ polymerization.

In this report, the term 'inhibition of polymerization' is used for both the decrease in FtsZ recovered in sedimentation or the decrease in light scattering that is observed when MinC-strep is included in the polymerization assay. In fact, from the EM images it seems that MinC-strep does not so much inhibit FtsZ polymer formation per se but rather influences the lateral arrangement of FtsZ polymers into parallel or bundled arrays. The fact that MinC-strep does not influence the GTP hydrolysis rate of FtsZ – which is tightly coupled to polymer formation [15] – also indicates that in the presence of MinC-strep FtsZ can still polymerize. These findings are in line with a paper on the effect of *E. coli* MinC on FtsZ that was published during preparation of this manuscript [18]. In this report, MalE-MinC was reported to destabilize lateral associations between FtsZ protofilaments without disturbing the total amount of FtsZ that is actually polymerized [18].

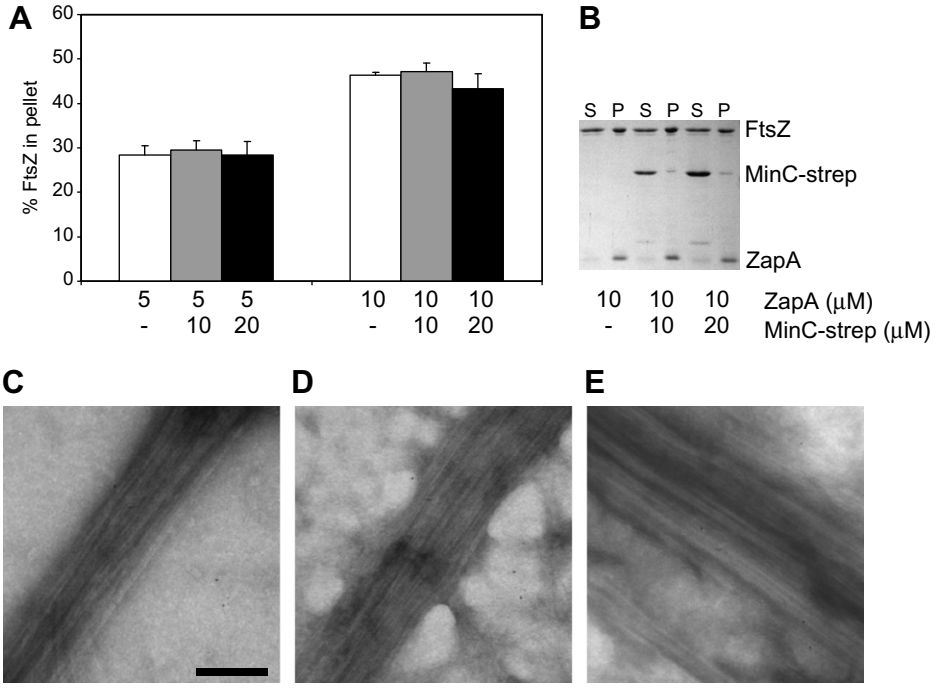

Fig. 4. ZapA counteracts the inhibitory effect of MinC. (A) Polymerization of FtsZ (10 μM) in HEPES, pH 7.5, with ZapA and MinC at concentrations indicated. Polymerization was analyzed by sedimentation as described (see text). (B) A representative gel with supernatant (S) and pellet (P) fractions for the 10 μM ZapA experiment. (C, D, E) Electron microscopy of the polymerisation reactions shows filaments for FtsZ (10 μM) polymerised with ZapA (10 μM) either in the absence (C) or presence of MinC at 10 μM (D) or 20 μM (E). Scale bar: 100 nm.

Light scattering and EM indicate that the organization of FtsZ into lateral arrays at pH 7.5 is not immediate, irrespective of the presence of MinC. Sedimentation shows that at higher pH less FtsZ can be recovered as polymers, also indicating that the total amount of polymerized FtsZ is lower at high pH and/or that the interaction between individual FtsZ filaments is weaker. Therefore, the enhanced effect of MinC at pH 7.5 may be the indirect result of the extra time that MinC has to interact with FtsZ polymers to block the association into lateral arrangements. Yet, a more likely explanation for the observed pH effect on MinC-strep is that MinC-strep has a higher affinity for FtsZ at pH 7.5 (as evidenced by the increase in scattering baseline signals). The sedimentation assay shows that after 5 min of polymerization MinC-strep already has maximally influenced the total amount of FtsZ polymers that can form lateral associations and thus be recovered by sedimentation. It seems that at physiological pH values, formation of lateral associations between *B. subtilis* FtsZ polymers is less immediate and thus more subject to regulation of additional factors, and that at least one such a factor, MinC, also has a higher affinity for FtsZ.

Although the overall effect of MinC on FtsZ seems very similar for the *B. subtilis* and *E. coli* proteins, some subtle differences do exist. *B. subtilis* MinC seems to be a less potent inhibitor of FtsZ polymerization as *E.coli* MinC can completely block FtsZ polymer sedimentation at a 1:1 ratio [5]. This block was observed at pH 6.5 (the internal pH of *E. coli* is in the range of 6.9–7.7 [31]). Completely blocked sedimentation at a FtsZ:MinC ratio of 1:1 was not observed with the *B. subtilis* proteins, however at pH 7.5 inhibition seemed maximal at MinC:FtsZ ratios of 1.5–2. A difference between this study and the reports on *E. coli* MinC is that *E. coli* MinC was purified fused to the 50 kDa MalE protein. One could imagine that MinC, which binds FtsZ and disturbs lateral interactions between FtsZ protofilaments probably through steric hindrance, is a more effective inhibitor when its size is considerably increased through the presence of MalE. *B. subtilis* FtsZ polymerization was found to be influenced by MalE alone, and MalE co-sedimented with FtsZ polymers (Fig. S1). Therefore, the MalE-fusion strategy was abandoned and a 10 aa strep-tag was used to purify *B. subtilis* MinC. As the conserved MinC19 mutation showed a reduced inhibitory effect in all polymerization assays, it is highly unlikely that the strep-tag alone influenced FtsZ polymerization.

ZapA is known to promote FtsZ bundling and to stabilize FtsZ polymers [28,29]. Strikingly, in the presence of ZapA the effect of MinC was completely abolished, as similar amounts of FtsZ were recovered in sedimentation assays with or without MinC, and the morphology of the polymers was not affected by MinC. In vivo experiments, in which *zapA* was shown to be essential when MinCD activity is not restricted to the poles through a *divIVA* deletion [28], already showed that ZapA can counteract, or protect FtsZ from, the inhibitory effects of the Min system. The presented results show that this counteracting effect is direct and does not require additional proteins. A similar effect for *E. coli* ZapA was recently reported [18].

In conclusion, this work shows that *B. subtilis* MinC influences FtsZ polymerization in a pH-dependent manner. Future studies will be aimed at the identification of the MinC binding site on FtsZ.

Acknowledgements: I would like to thank Jeremy Bartosiák-Jentys and Viola Kooij for technical assistance during the initial stages of this study, Joen Luirink, Jeff Errington, Daniel Haeusser and Petra Levin for critical reading of the manuscript, and Jan van Minnen for help with electron microscopy. The anonymous referees are thanked for helpful suggestions that have improved the manuscript.

This work was supported by a VENI grant from the Research Council for Earth and Life Sciences (ALW) with financial aid from the Netherlands Organization for Scientific Research (NWO).

Appendix A. Supplementary data

Supplementary data associated with this article can be found, in the online version, at doi:10.1016/j.febslet.2008.06.038.

References

[1] Goehring, N.W. and Beckwith, J. (2005) Diverse paths to midcell: assembly of the bacterial cell division machinery. Curr. Biol. 15, R514–R526.
[2] Errington, J., Daniel, R.A. and Scheffers, D.-J. (2003) Cytokinesis in bacteria. Microbiol. Mol. Biol. Rev. 67, 52–65.
[3] Rothfield, L., Taghbalout, A. and Shih, Y.L. (2005) Spatial control of bacterial division-site placement. Nat. Rev. Microbiol. 3, 959–968.
[4] de Boer, P.A.J., Crossley, R.E. and Rothfield, L.I. (1989) A division inhibitor and a topological specificity factor coded for by the minicell locus determine proper placement of the division septum in *E. coli*. Cell 56, 641–649.
[5] Hu, Z., Mukherjee, A., Pichoff, S. and Lutkenhaus, J. (1999) The MinC component of the division site selection system in *Escherichia coli* interacts with FtsZ to prevent polymerization. Proc. Natl. Acad. Sci. USA 96, 14819–14824.
[6] Hu, Z. and Lutkenhaus, J. (2001) Topological regulation of cell division in *E. coli* spatiotemporal oscillation of MinD requires stimulation of its ATPase by MinE and phospholipid. Mol. Cell 7, 1337–1343.
[7] Hu, Z., Saez, C. and Lutkenhaus, J. (2003) Recruitment of MinC, an inhibitor of Z-ring formation, to the membrane in *Escherichia coli*: role of MinD and MinE. J. Bacteriol. 185, 196–203.
[8] Suefuji, K., Valluzzi, R. and RayChaudhuri, D. (2002) Dynamic assembly of MinD into filament bundles modulated by ATP, phospholipids, and MinE. Proc. Natl. Acad. Sci. USA 99, 16776–16781.
[9] Edwards, D.H. and Errington, J. (1997) The *Bacillus subtilis* DivIVA protein targets to the division septum and controls the site specificity of cell division. Mol. Microbiol. 24, 905–915.
[10] Marston, A.L., Thomaides, H.B., Edwards, D.H., Sharpe, M.E. and Errington, J. (1998) Polar localization of the MinD protein of *Bacillus subtilis* and its role in selection of the mid-cell division site. Genes Dev. 12, 3419–3430.
[11] Raskin, D.M. and De Boer, P.A.J. (1999) Rapid pole-to-pole oscillation of a protein required for directing division to the middle of *Escherichia coli*. Proc. Natl. Acad. Sci. USA 96, 4971–4976.
[12] Raskin, D.M. and De Boer, P.A.J. (1999) MinDE-dependent pole-to-pole oscillation of division inhibitor MinC in *Escherichia coli*. J. Bacteriol. 181, 6419–6424.
[13] Howard, M. (2004) A mechanism for polar protein localization in bacteria. J. Mol. Biol. 335, 655–663.
[14] Meinhardt, H. and de Boer, P.A. (2001) Pattern formation in *Escherichia coli*: a model for the pole-to-pole oscillations of Min proteins and the localization of the division site. Proc. Natl. Acad. Sci. USA 98, 14202–14207.
[15] Scheffers, D.-J., de Wit, J.G., den Blaauwen, T. and Driessen, A.J.M. (2002) GTP hydrolysis of cell division protein FtsZ: evidence that the active site is formed by the association of monomers. Biochemistry 41, 521–529.
[16] Hu, Z. and Lutkenhaus, J. (2000) Analysis of MinC reveals two independent domains involved in interaction with MinD and FtsZ. J. Bacteriol. 182, 3965–3971.

[17] Shiomi, D. and Margolin, W. (2007) The C-terminal domain of MinC inhibits assembly of the Z ring in *Escherichia coli*. J. Bacteriol. 189, 236–243.
[18] Dajkovic, A., Lan, G., Sun, S.X., Wirtz, D. and Lutkenhaus, J. (2008) MinC spatially controls bacterial cytokinesis by antagonizing the scaffolding function of FtsZ. Curr. Biol. 18, 235–244.
[19] Cordell, S.C., Anderson, R.E. and Löwe, J. (2001) Crystal structure of the bacterial cell division inhibitor MinC. EMBO J. 20, 2454–2461.
[20] Oliva, M.A., Trambaiolo, D. and Löwe, J. (2007) Structural insights into the conformational variability of FtsZ. J. Mol. Biol. 373, 1229–1242.
[21] Sambrook, J., Fritsch, E.F. and Maniatis, T. (1989) Molecular Cloning: A Laboratory Manual, Cold Spring Harbor Laboratory Press, Cold Spring Harbor.
[22] Wang, X. and Lutkenhaus, J. (1993) The FtsZ protein of *Bacillus subtilis* is localized at the division site and has GTPase activity that is dependent upon FtsZ concentration. Mol. Microbiol. 9, 435–442.
[23] Scheffers, D.-J., den Blaauwen, T. and Driessen, A.J.M. (2000) Non-hydrolysable GTP-γ-S stabilizes the FtsZ polymer in a GDP-bound state. Mol. Microbiol. 35, 1211–1219.
[24] Mukherjee, A. and Lutkenhaus, J. (1999) Analysis of FtsZ assembly by light scattering and determination of the role of divalent metal cations. J. Bacteriol. 181, 823–832.
[25] Haeusser, D.P., Schwartz, R.L., Smith, A.M., Oates, M.E. and Levin, P.A. (2004) EzrA prevents aberrant cell division by modulating assembly of the cytoskeletal protein FtsZ. Mol. Microbiol. 52, 801–814.
[26] Singh, J.K., Makde, R.D., Kumar, V. and Panda, D. (2007) A membrane protein, EzrA, regulates assembly dynamics of FtsZ by interacting with the C-terminal tail of FtsZ. Biochemistry 46, 11013–11022.
[27] Waxman, P.G., del Campo, A.A., Lowe, M.C. and Hamel, E. (1981) Induction of polymerization of purified tubulin by sulfonate buffers. Marked differences between 4-morpholineethanesulfonate (MES) and 1,4-piperazineethanesulfonate (Pipes). Eur. J. Biochem. 120, 129–136.
[28] Gueiros-Filho, F.J. and Losick, R. (2002) A widely conserved bacterial cell division protein that promotes assembly of the tubulin-like protein FtsZ. Genes Dev. 16, 2544–2556.
[29] Low, H.H., Moncrieffe, M.C. and Löwe, J. (2004) The crystal structure of ZapA and its modulation of FtsZ polymerisation. J. Mol. Biol. 341, 839–852.
[30] Breeuwer, P., Drocourt, J., Rombouts, F.M. and Abee, T. (1996) A novel method for continuous determination of the intracellular ph in bacteria with the internally conjugated fluorescent probe 5 (and 6-)-carboxyfluorescein succinimidyl ester. Appl. Environ. Microbiol. 62, 178–183.
[31] Riondet, C., Cachon, R., Waché, Y., Alcaraz, G. and Diviès, C. (1997) Measurement of the intracellular pH in *Escherichia coli* with the internally conjugated fluorescent probe 5- (and 6-)carboxyfluorescein succinimidyl ester. Biotechnol. Tech. 11, 735–738.
[32] Studier, F.W., Rosenberg, A.H., Dunn, J.J. and Dubendorff, J.W. (1990) Use of T7 RNA polymerase to direct expression of cloned genes. Meth. Enzymol. 185, 60–89.
[33] Lewis, P.J. and Marston, A.L. (1999) GFP vectors for controlled expression and dual labelling of protein fusions in *Bacillus subtilis*. Gene 227, 101–109.